Updated assessment of the South African sardine resource using data from 1984-2020

C.L. de Moor*

Correspondence email: *carryn.demoor@uct.ac.za*

A quantitative assessment of the South African sardine resource has been updated to include data from 1984 to 2020. This two mixing-component hypothesis assumes no stock recruitment relationship during conditioning. The west component abundance remains at a low level, but the spawner biomass is estimated to be higher than that estimated a year ago. These results have shown that the model is sensitive to the inclusion of parasite prevalence-at-length data and further investigation into the most appropriate manner with which these data should be included in the model is warranted. Further sensitivity testing and the consideration of alternative hypotheses is required before a 'baseline' assessment can be selected.

Keywords: assessment, population dynamics, parasite prevalence-at-length, sardine

Introduction

This document presents results for a 'simple updated' assessment of South African sardine, using data from 1984-2020. The assessment assumes the sardine population consists of two mixing 'components', with a west component distributed west of Cape Agulhas and a south component distributed south-east of Cape Agulhas. This hypothesis assumes there is movement of fish from the west component into the south component and a small contribution of south component spawning to west component recruitment. The former is modelled by an annually-varying proportion of west component sardine moving to form part of the south component while the latter is modelled by assuming a time-invariant 8% of south component spawner biomass contributes to west component effective spawner biomass.

Data and Population Dynamics Model

The population dynamics model for the South African sardine resource is the same as that detailed in Appendix A of de Moor (2020a)[1], extended for an additional year.

The data used in this assessment are listed in de Moor *et al*. (2021). The prevalence-at-length data collected from annual acoustic surveys were originally included in the assessment model to help improve the confidence with which movement (in particular) was estimated (de Moor *et al*. 2017, Figure 1). The inclusion of a time series of parasite prevalence-at-length from commercial catches (aligned with the four annual model quarters) as well as parasite intensity-at-length data into the likelihood of the model has been proposed many times, but not yet undertaken due to time constraints. Given low samples of large fish on the south coast in the November 2019 and 2020 acoustic surveys, van der Lingen (2021) proposed that samples from commercial catches collected between September and November of these years be added to the samples from the acoustic survey off the south coast in 2019 and from the west and south coasts in 2020. Further work is still ongoing to update van der Lingen (2021) such that the comparisons of historical prevalence-at-length from survey and commercial data are undertaken using samples from the same area and time period. In the meantime, the assessment is run both with and without the prevalence-at-length data from survey and/or commercial samples in 2019 and 2020 to consider the impact of including commercial data for two years only.

* MARAM (Marine Resource Assessment and Management Group), Department of Mathematics and Applied Mathematics, University of Cape Town, Rondebosch, 7701, South Africa.

[1] With the adjustment to the growth curve for ages < 6 months for both south and west components.

Results and Discussion

Table 1 lists the changes in model fits to the data and estimates of final year biomass depending on which parasite prevalence-at-length data are used to condition the model. Including the prevalence-at-length data sampled from acoustic surveys in the model results in some improvement in the estimation of the annual proportion moving in the past decade, at the expense of fitting other data (Figures 2a,c, Table 1). In some years, the confidence intervals are decreased substantially. The confidence intervals in the estimate of the proportion moving in 2013 are mutually exclusive between including or excluding the prevalence data, which merits further investigation (this was not observed by de Moor *et al*. 2017, see Figure 1). The inclusion of the 2019 prevalence-at-length data only results in a substantial change in estimated movement in 2019 (Figure 2a), with a substantial increase/decrease in $B^S_{w,2019}$ / $B^S_{s,2019}$, with a smaller increase/decrease in $B^S_{w,2020}$ / $B^S_{s,2020}$. The inclusion of 2020 prevalence-at-length data results in a substantial increase in the estimated biomass in November 2020, with little change to the November likelihood (Table 1). The Hessian-based confidence interval of the estimate of the proportion moving in November 2020 when the additional commercial samples are included, only just includes the best estimate achieved without the 2020 commercial samples (Figures 2b,c).

While narrowing of the confidence intervals of some estimated parameters with little deterioration in the fit to the acoustic survey data was expected *a priori* by including the prevalence-at-length data in the model (de Moor *et al*. 2017), these results indicate there may be some conflict between the data used to condition this model and this should be explored further.

The model is able to fit the survey estimates of abundance well in most years (Figures 3 and 4). The years for which the model predicted value exceeded the 95% confidence interval of the survey estimate typically corresponded to years for which there is conflicting information between the November biomass and May/June recruit surveys. The relatively high model predicted recruitment on the south coast in May/June 2018 to 2020 are now primarily informed by length frequency data given the absence of survey estimates of recruitment in these recent years. There is a deterioration in the model's ability to fit these survey data in the most recent three years when prevalence-at-length data are included in the likelihood.

The model fit to the survey length frequencies (Figures 6, 7) and commercial length frequencies (Figures 9 and 10) is relatively good, with little noticeable change to that achieved by de Moor (2020a), and with similar survey and commercial selectivities to that estimated by de Moor (2020a) (Figures 5 and 8). The fit to survey and commercial length frequencies improves substantially when the prevalence-at-length data are excluded from the likelihood (Figures 7, 10).

Figure 11 shows the growth curves which are modelled to vary by cohort. For model iv) the average $t_{0,j,y}$ for the von Bertalanffy growth curves for the south component is 0.25 (close to November) with a maximum difference in $t_{0,j,y}$ between cohorts of approximately 8 months. Even with an adjustment to the growth curve for the west component, the average $t_{0,j,y}$ is approximately 7 months before November, with a maximum difference in $t_{0,j,y}$ between cohorts of about 7.5 months. These ranges are similar to that of de Moor (2020a), and as previously suggested further alternative adjustments to the growth curve should be explored. However, for model i) which excludes the parasite data from the likelihood, the the average $t_{0,j,y}$ for the von Bertalanffy growth curves for the west component is 0.18 (approx. 2 months after 1 November) with a maximum difference in $t_{0,j,y}$ between cohorts of approximately 6 months, while the average $t_{0,j,y}$ for the south component corresponds with 1 October. These ranges

correspond closer to that expected a priori, i.e. a birth date close to 1 November for the west component and earlier (due to winter spawning) for the south component. Figure 12 shows the length-at-age distributions for one example year.

The model estimated annual proportion of west component sardine infected by the "tetracotyle" type digenean endoparasite is shown in Figure 13. The model fit to the parasite prevalence data between 2010 and 2016 is relatively unchanged from that of de Moor (2020a), but is updated in 2018 to 2020 with the addition of new data (Figure 14a). The change in prevalence-at-length in 2019 and 2020, with the inclusion of samples from commercial catches between September and November can be seen by comparing Figures 14a and 14b.

The model estimated November recruitment is plotted against spawner biomass and effective spawner biomass in Figure 15, indicating the low west component [effective] spawner biomass and recruitment in recent years. The west component effective spawner biomass includes 8% of the south component spawner biomass. The proportion of this effective west component spawner biomass that consists of south component spawner biomass is estimated to be high after the turn of the century and again in recent years, reaching 57% in 2019 (Figure 16). This reflects the low current west component spawner biomass.

The updated and extended time series of data has some correction to the de Moor (2020a) estimate of November biomass in 2019 (Figures 1 and 17) and west component recruitment in May/June 2019 (November 2018) (Figures 2 and 16). However, this correction is not as extensive as that noted a year ago (de Moor 2020a). This model option iv) estimates the effective west and south component spawner biomasses to be 39 000t and 168 000t in November 2020, respectively, while model option i) estimates the effective west and south component spawner biomasses to be 29 000t and 186 000t.

Figure 18 shows the historical harvest proportion on the sardine, which has often been substantially higher on the west component than on the south component.

In Summary

This document has presented an updated assessment of South African sardine. For many parameters and model outputs, only results at the joint posterior mode have been provided thus far, and readers are reminded that there is estimation error about these values.

The assessment model i) estimates the west component biomass in November 2020 to be about 79 000t - 18% of the historical (1984-2019) average. The west component spawner biomass is estimated to be about 13 000t (24% of the historical average) and the effective spawner biomass is estimated to be 29 000t (42% of the historical average). This is a lower biomass, but higher spawner biomass than estimated last year (de Moor 2020a). The corresponding values from assessment model iv) are 187 500t (44% of historical biomass), 24 000t (43% of historical spawner biomass) and 39 000t (53% of historical effective spawner biomass) which are all higher than that estimated for November 2019 by de Moor (2020a).

The assessment model iv) estimates the south component biomass in November 2020 to be about 724 000t which is above the historical average and the south component spawner biomass and effective spawner biomass are estimated to be at 99% of the historical average at 202 000t and 186 000t, respectively. The assessment model iv) estimates the south component biomass in

November 2020 to be about 483 500t which is 90% of the historical average and the south component spawner biomass and effective spawner biomass are estimated to be at 88% of the historical average at 182 000t and 167 500t, respectively.

It is expected that a range of sensitivity testing as well as alternative hypothesis will be considered prior to a baseline(s) being selected for the Operating Models that will be used to simulation test OMP-22. However, this initial updated assessment is presented now to be used to provide 'ad hoc' management advice for sardine (in the same manner as that followed the previous two years), given that the OMP is not being used following the declaration of Exceptional Circumstances for sardine.

References

de Moor CL. 2020a. South African sardine assessment posterior distributions and sensitivity tests. DEFF: Branch Fisheries Document FISHERIES/2020/DEC/SWG-PEL/138.

de Moor CL. 2020b. Final baseline assessment of the South African sardine resource using data from 1984-2018. DEA: Branch Fisheries Document FISHERIES/2020/MAR/SWG-PEL/28.

de Moor CL, Butterworth DS and van der Lingen CD. 2017. The quantitative use of parasite data in multistock modelling of South African sardine (Sardinops sagax). *Can. J. Fish. Aquat. Sci*. 74:1895-1903.

de Moor CL, Merkle D, Coetzee J and van der Lingen C. 2021. The data used in the 2021 sardine assessment. DEFF: Branch Fisheries Document FISHEREIS/2021/APR/SWG-PEL/22.

van der Lingen CD. 2021. Comparing prevalence-at-length plots for western and southern sardine from Pelagic Biomass Survey and commercial catch samples, 2010-2018. DEFF: Branch Fisheries Document FISHERIES/2021/MAR/SWG-PEL/15.

Table 1. The contributions to the objective function from likelihood and prior components, together with the associated estimated survey bias parameters, $k^S_{j,N}$ and $k^S_{j,r}$, model predicted biomass in 2018-2020, $B^S_{j,y}$, and model predicted spawner biomass in 2018-2020, $B^{sp,S}_{j,y}$. The Hessian-based CV is included in parentheses for $B^S_{w,2020}$.

Option	Prevalence Included In Likelihood															
	2010-2018 from surveys	2019 from survey	2020 from survey	2019 from commercial	2020 from commercial	Obj fn	$-lnL$	$-lnL^{Nov}$	$-lnL^{rec}$	$-lnL^{com\ propl}$	$-lnL^{sur\ propl}$	$-lnL^{prev}$	$ln(k^S_{ac})$	$move_{y,1}$	η^t_y	$\bar{l}_{1,y}$	$k^S_{j,N}$	$k^S_{w,r}$
i)	x	x	x	x	x	-705.30	-771.83	56.32	38.56	-458.39	-408.32	3533.94	-1.401	-32.74	-20.47	121.04	0.75	0.48
ii)	Y	x	x	x	x	978.91	904.59	62.54	41.18	-450.88	-398.61	1650.37	-1.33	-32.06	-13.44	120.81	0.77	0.58
iii)	Y	Y	x	x	x	1125.42	1051.58	63.00	40.49	-449.38	-393.88	1791.34	-1.28	-31.80	-14.22	120.76	0.77	0.62
iv)	Y	Y	Y	x	x	1211.03	1136.88	63.08	40.62	-449.34	-394.47	1876.99	-1.25	-31.78	-13.87	120.76	0.78	0.62
v)	Y	Y	x	Y	x	1126.73	1052.16	63.06	40.41	-449.20	-394.45	1792.33	-1.29	-31.80	-13.47	120.74	0.77	0.63
vi)	Y	Y	Y	Y	x	1213.01	1138.61	63.10	40.74	-429.34	-395.78	1879.89	-1.23	-32.09	-13.93	120.75	0.78	0.63
vii)	Y	Y	Y	Y	Y	1363.32	1288.04	63.85	40.38	-449.08	-393.35	2026.24	-1.22	-31.72	-12.88	120.74	0.78	0.63
	2010-2018 from surveys	2019 from survey	2020 from survey	2019 from commercial	2020 from commercial	$B^S_{w,2018}$	$B^S_{w,2019}$	$B^S_{w,2020}$	$B^{sp,S}_{w,2018}$	$B^{sp,S}_{w,2019}$	$B^{sp,S}_{w,2020}$	$B^S_{s,2018}$	$B^S_{s,2019}$	$B^S_{s,2020}$	$B^{sp,S}_{s,2018}$	$B^{sp,S}_{s,2019}$	$B^{sp,S}_{s,2020}$	
i)	x	x	x	x	x	35.6	45.3	79.1 (0.92)	8.5	6.8	9.4	308.8	450.2	723.8	132.9	135.9	213.6	
ii)	Y	x	x	x	x	51.5	64.2	73.3 (0.87)	6.5	1.1	5.3	254.2	434.6	715.9	132.9	123.0	285.7	
iii)	Y	Y	x	x	x	36.6	149.7	92.8*	6.6	6.8	14.1	230.5	279.1	590.1	121.8	106.3	209.1	
iv)	Y	Y	Y	x	x	31.5	113.1	187.6 (0.56)	7.6	6.6	24.1	237.7	271.6	483.5	122.9	110.4	182.2	
v)	Y	Y	x	Y	x	35.7	155.2	90.8 (0.86)	6.6	6.3	12.9	248.5	280.5	588.1	122.6	116.4	202.5	
vi)	Y	Y	Y	Y	x	29.9	119.10	192.2 (0.56)	7.7	6.0	23.8	252.7	277.4	485.9	123.4	119.7	179.5	
vii)	Y	Y	Y	Y	Y	28.5	122.6	215.9 (0.46)	8.5	5.3	23.2	250.7	258.7	434.4	121.3	117.9	166.1	

*Non positive definite Hessian

Fig. 8. The posterior median and 95% probability intervals of proportions of 1-year-olds estimated to move from the west to the south stock each November from 2008 to 2015, for S_{with} (diamonds) and $S_{without}$ (circles). Results for all years are shown in the online supplementary material (Fig. S6[2]).

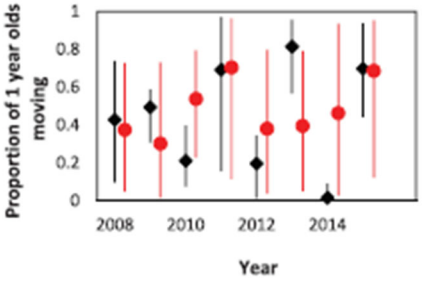

Figure 1. Figure 8 of de Moor et al. (2017) showing the improvement in the ability for the model to estimate annual proportions moving given the inclusion of parasite prevalence-at-length data in the likelihood.

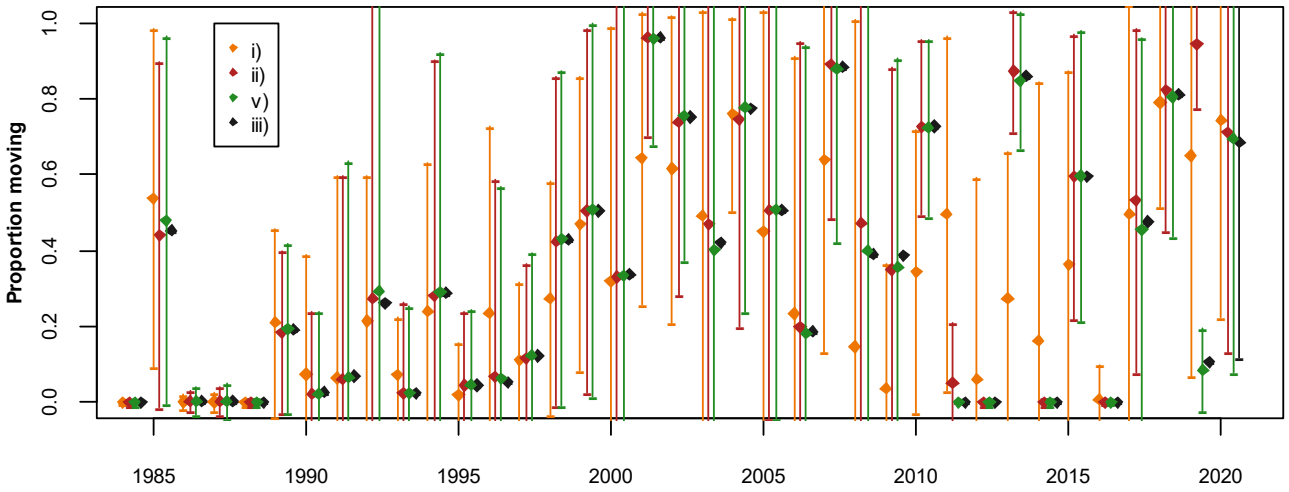

Figure 2a. The model estimated annual proportion (with 95% Hessian-based confidence interval for options i), ii), v)) of west component 1-year olds that move to the south component for model scenarios which exclude prevalence-at-length data in 2020.

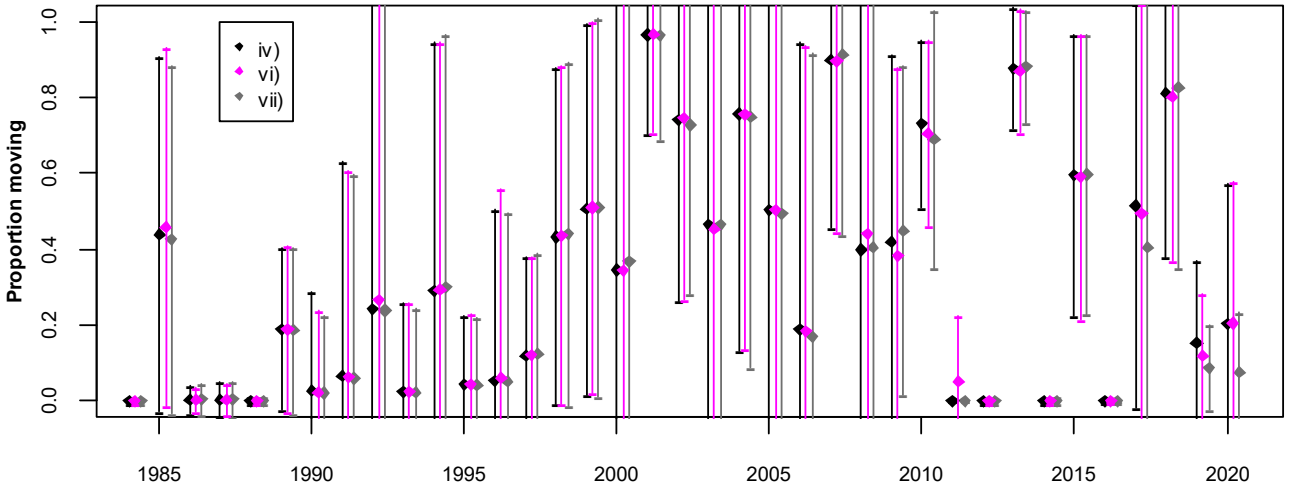

Figure 2b. The model estimated annual proportion (with 95% Hessian-based confidence interval) of west component 1-year olds that move to the south component for model scenarios which include prevalence-at-length data in 2020.

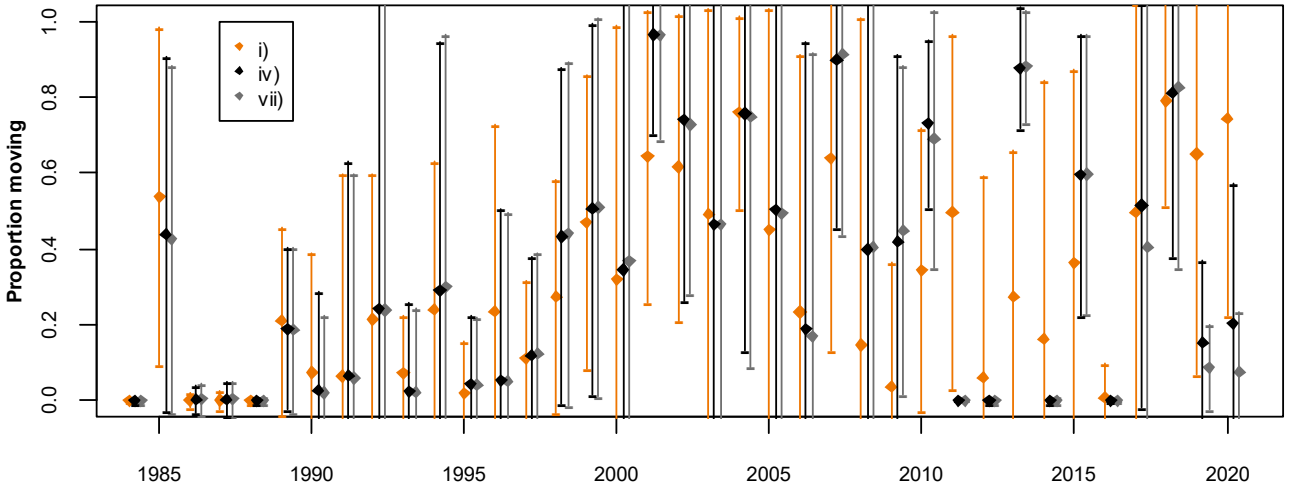

Figure 2c. The model estimated annual proportion (with 95% Hessian-based confidence interval) of west component 1-year olds that move to the south component for model scenarios which i) exclude all prevalence-at-length data, iv) include all prevalence-at-length data from samples collected from acoustic surveys and vii) additionally include prevalence-at-length data from samples collected from commercial catches in 2019 (south only) and 2020.

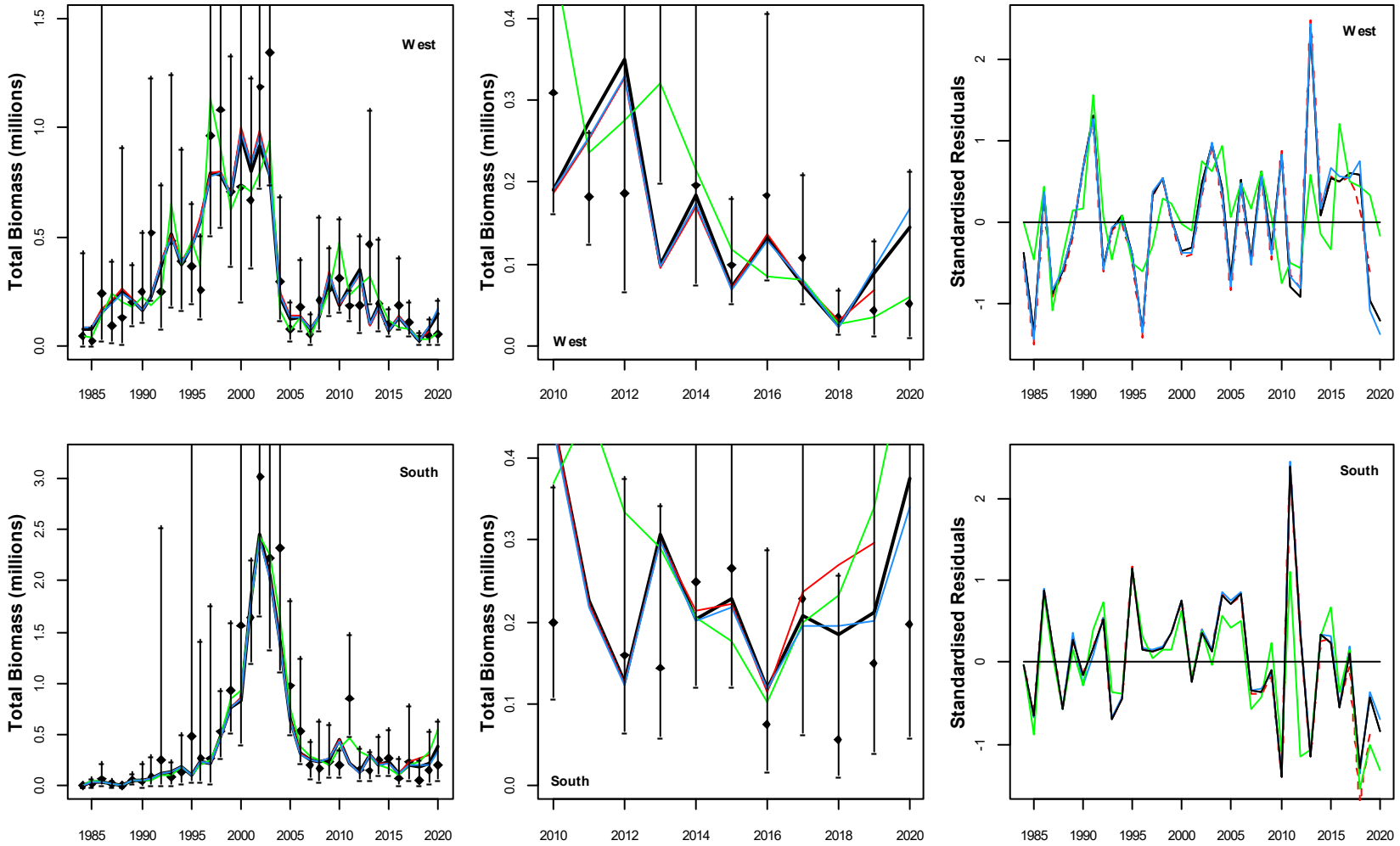

Figure 3. Acoustic survey estimated and model predicted November sardine total biomass from 1984 to 2020 for model option iv) (black) compared to i) (green) and vii) (blue). The observed indices are shown with 95% confidence intervals. The centre plot shows only the most recent 11 years of the left hand plot. The standardised residuals (i.e. the residual divided by the corresponding standard deviation, including additional variance where appropriate) from the fits are given in the right hand plots. The red lines indicate the November biomass predicted by the baseline model of de Moor (2020a) and associated residuals.

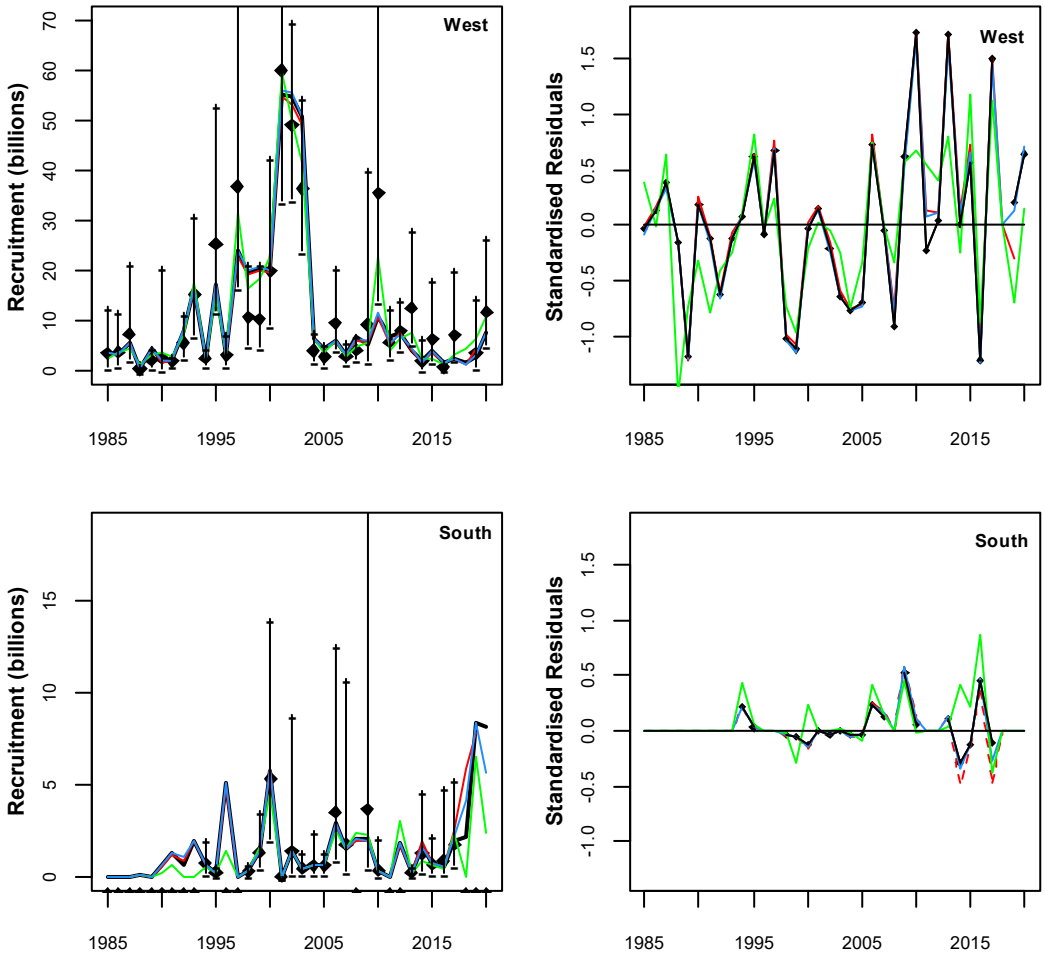

Figure 4. Acoustic survey estimated and model predicted sardine recruitment numbers from May/June 1985 to 2020 for model option iv) (black) compared to i) (green) and vii) (blue). There was no survey observation in 2018; the model predicted value corresponds to the recruitment predicted at 8th June 2018 which is the average start date of the survey from 2016, 2017 and 2019 surveys. The survey indices are shown with 95% confidence intervals. The standardised residuals from the fit are given in the right hand plots. The red lines indicate the May recruitment predicted by baseline model of de Moor (2020a) and associated residuals.

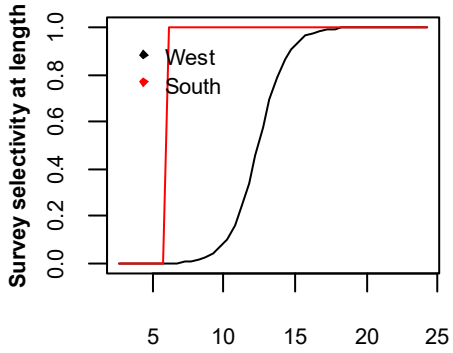

Figure 5. The model estimated November survey selectivity at length for model option iv).

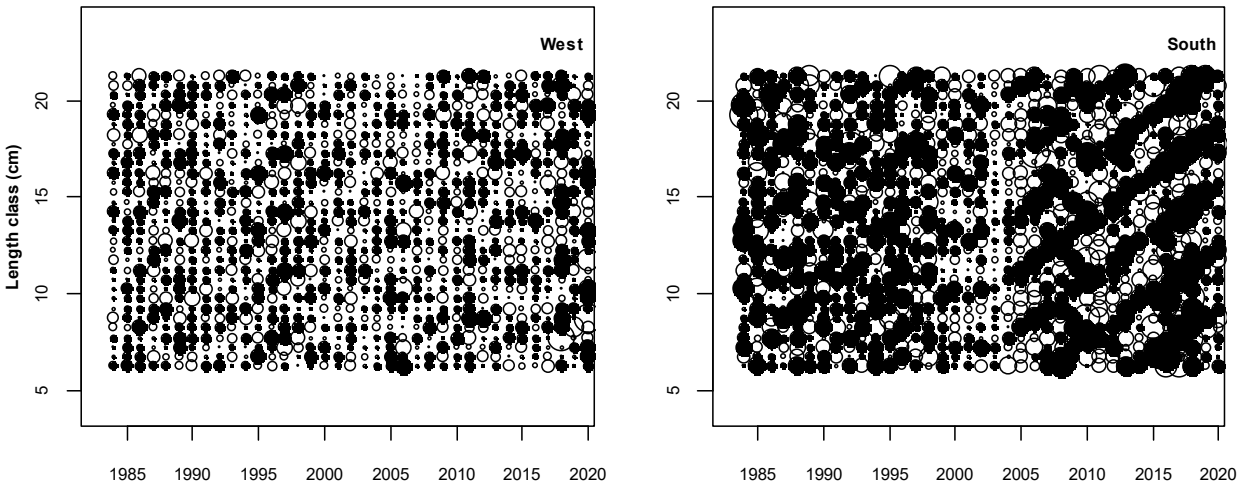

Figure 6. Residuals from the fit of the model predicted proportions-at-length in the November survey to the hydroacoustic survey estimated proportions for model option iv).

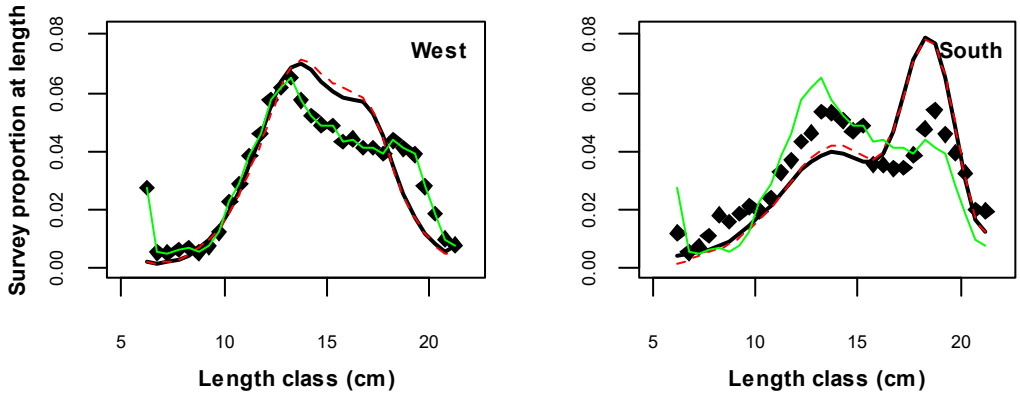

Figure 7. Average (over all years) model predicted and observed proportion-at-length in the November survey for model option iv) (black) compared to i) (green), with the red lines indicating that predicted by baseline model of de Moor (2020a).

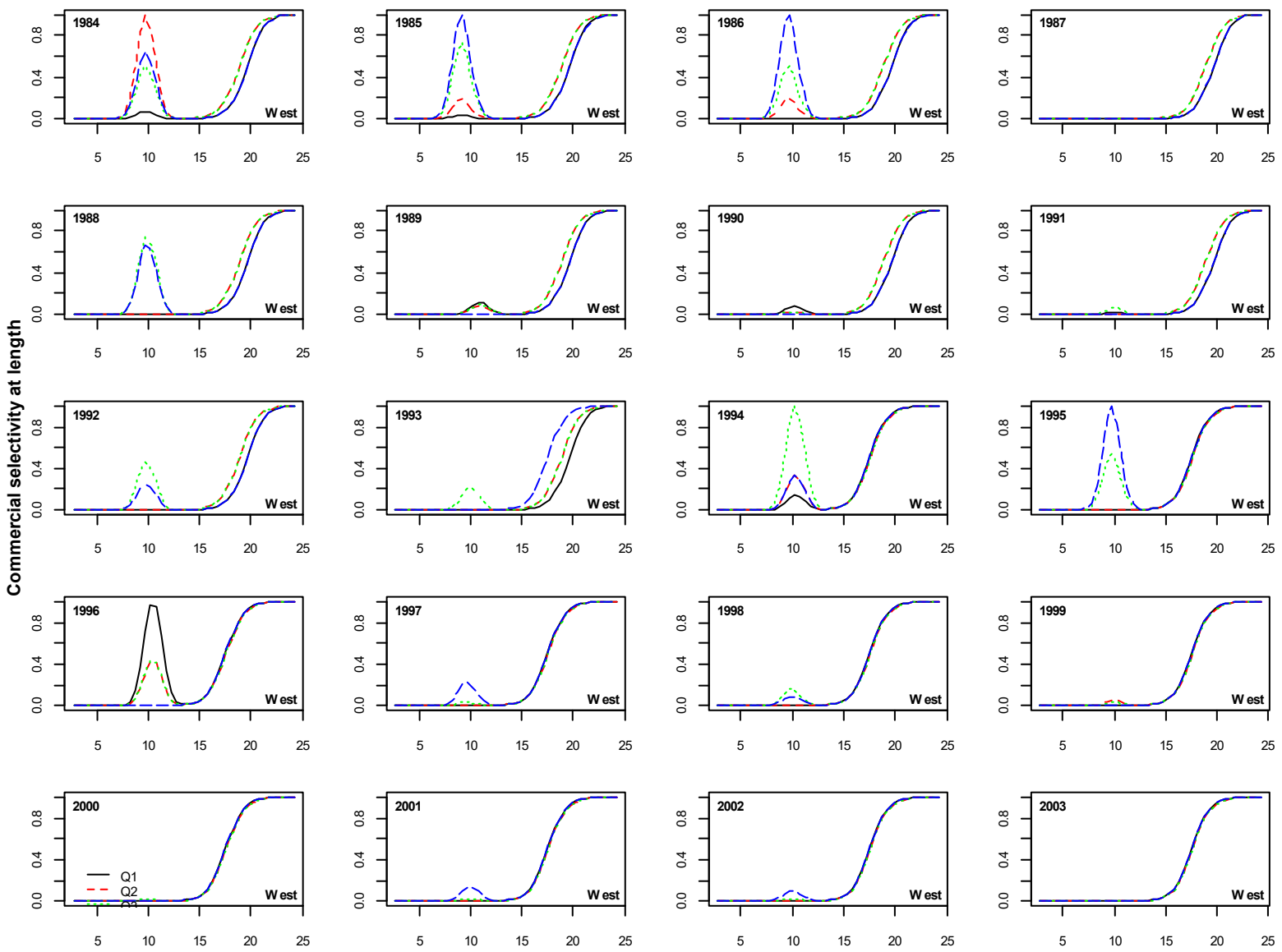

Figure 8. The model estimated commercial selectivity at length for model option iv).

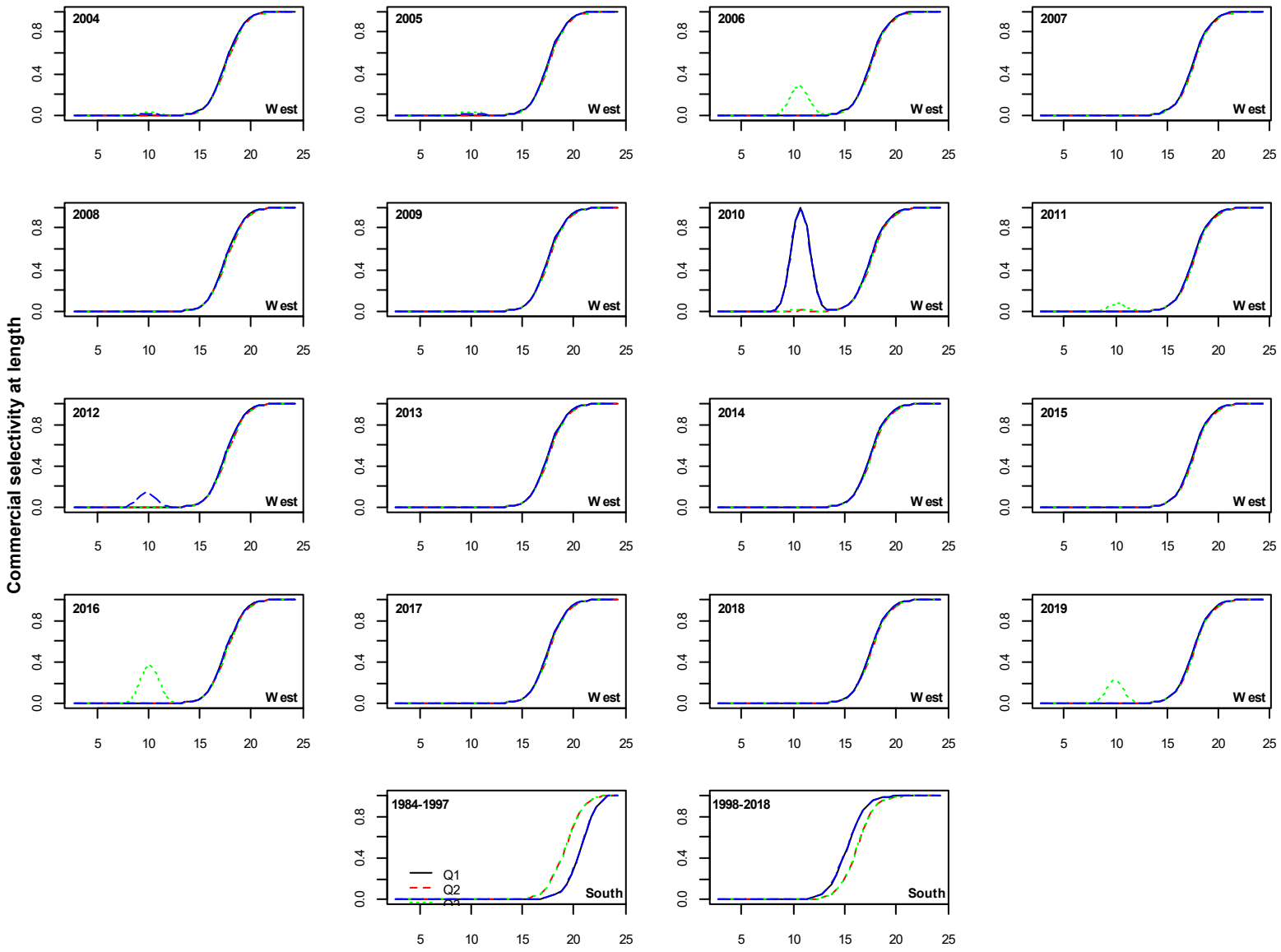

Figure 8 (continued).

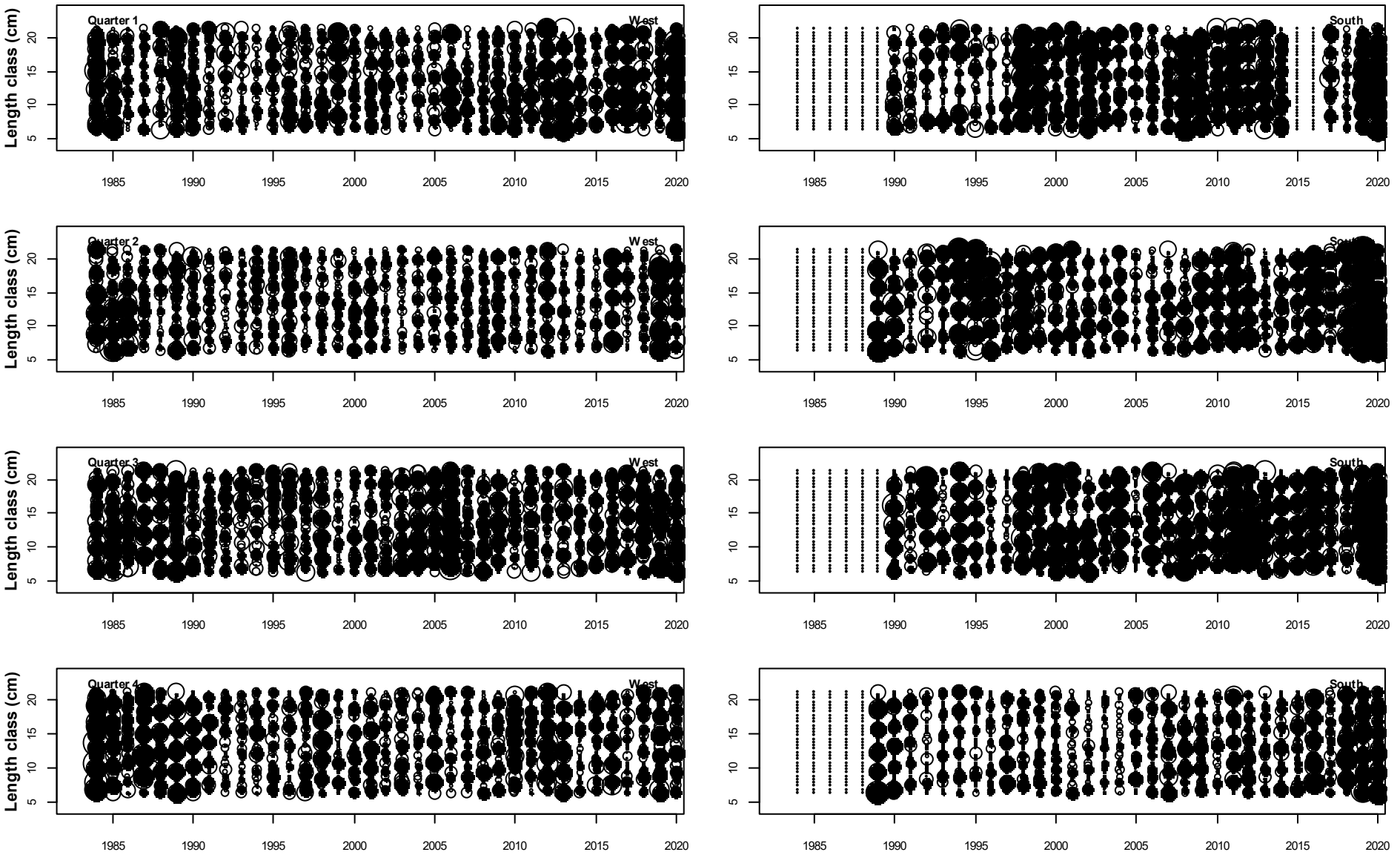

Figure 9. Residuals from the fit of the model predicted proportions-at-length in the quarterly commercial catch to the observed proportions for model option iv).

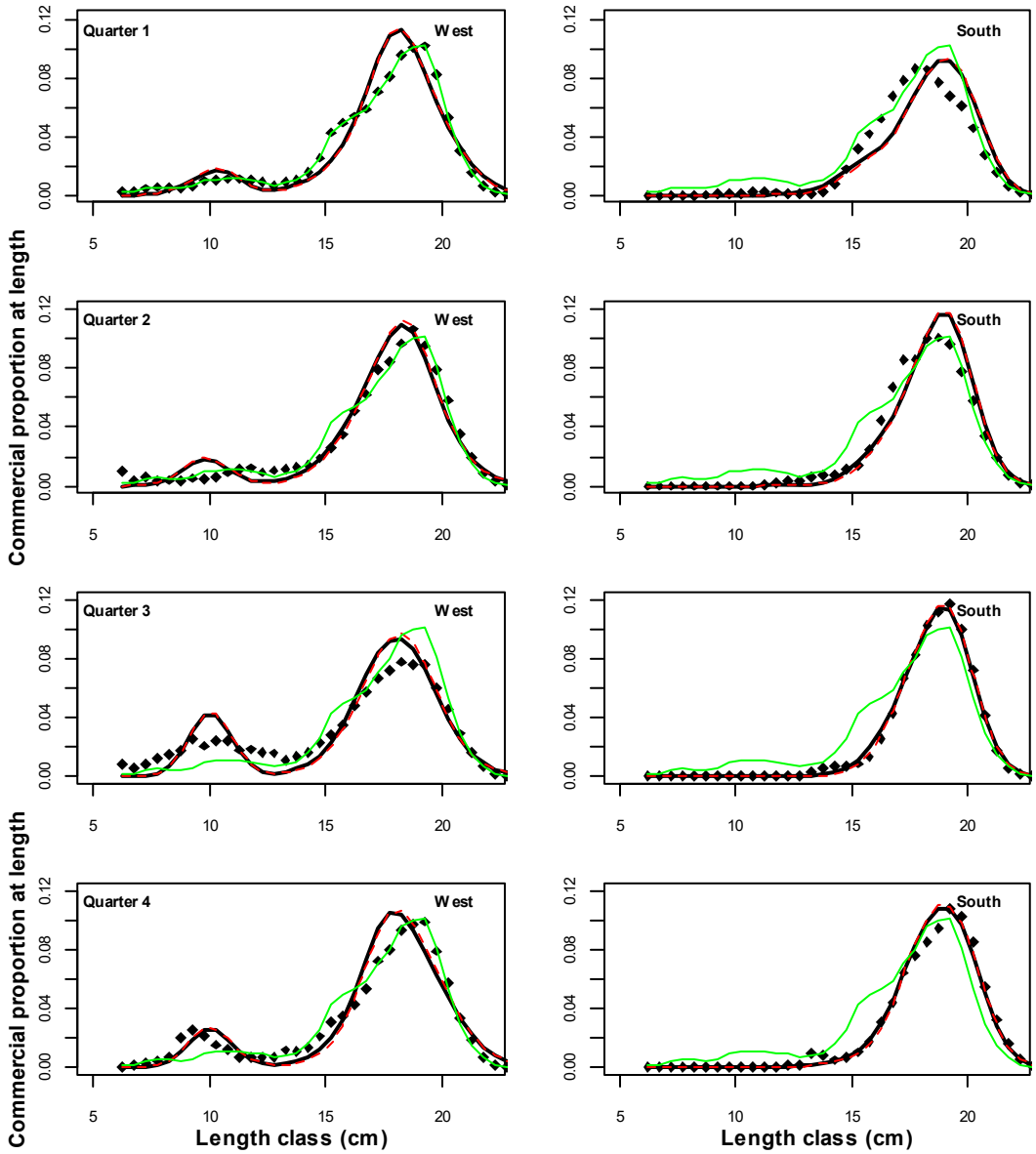

Figure 10. Average (over all years) quarterly model predicted and observed proportion-at-length in the commercial catch for model option iv) (black) compared to i) (green), with the red lines indicating that predicted by baseline model of de Moor (2020a).

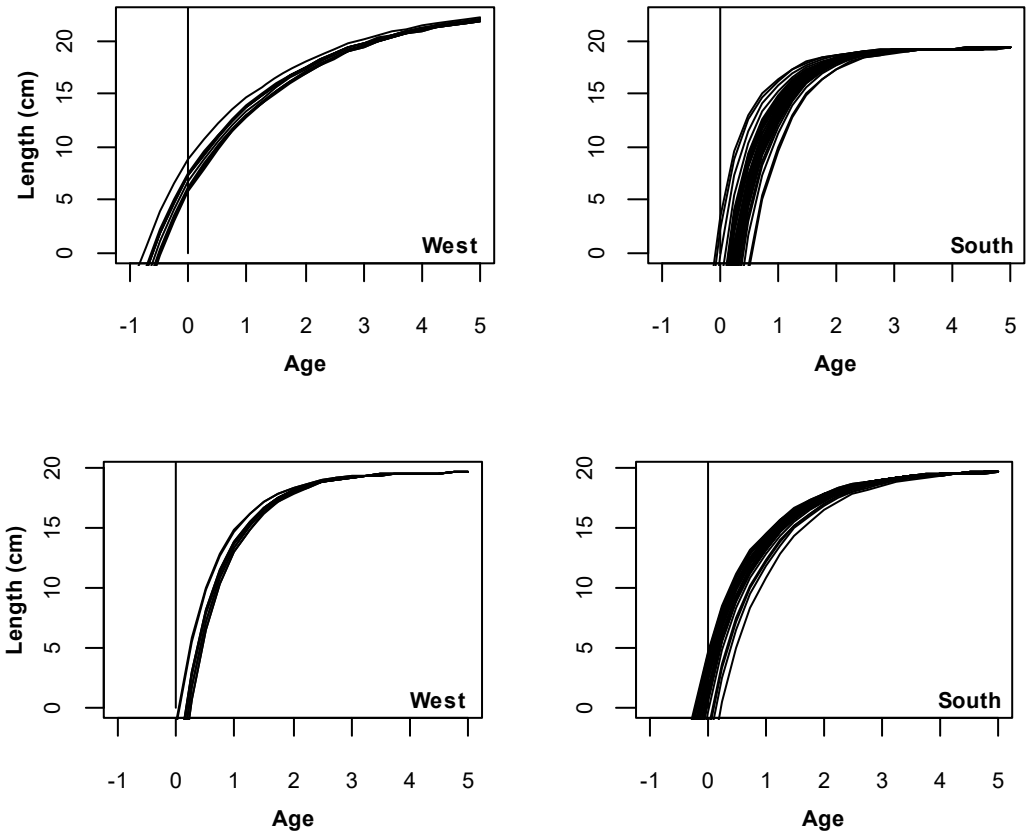

Figure 11. The von Bertalanffy growth curves (by cohort) estimated for model option iv) (above) and model option i) (below) by allowing for auto-correlated residuals for the variation about the age at which length is zero.

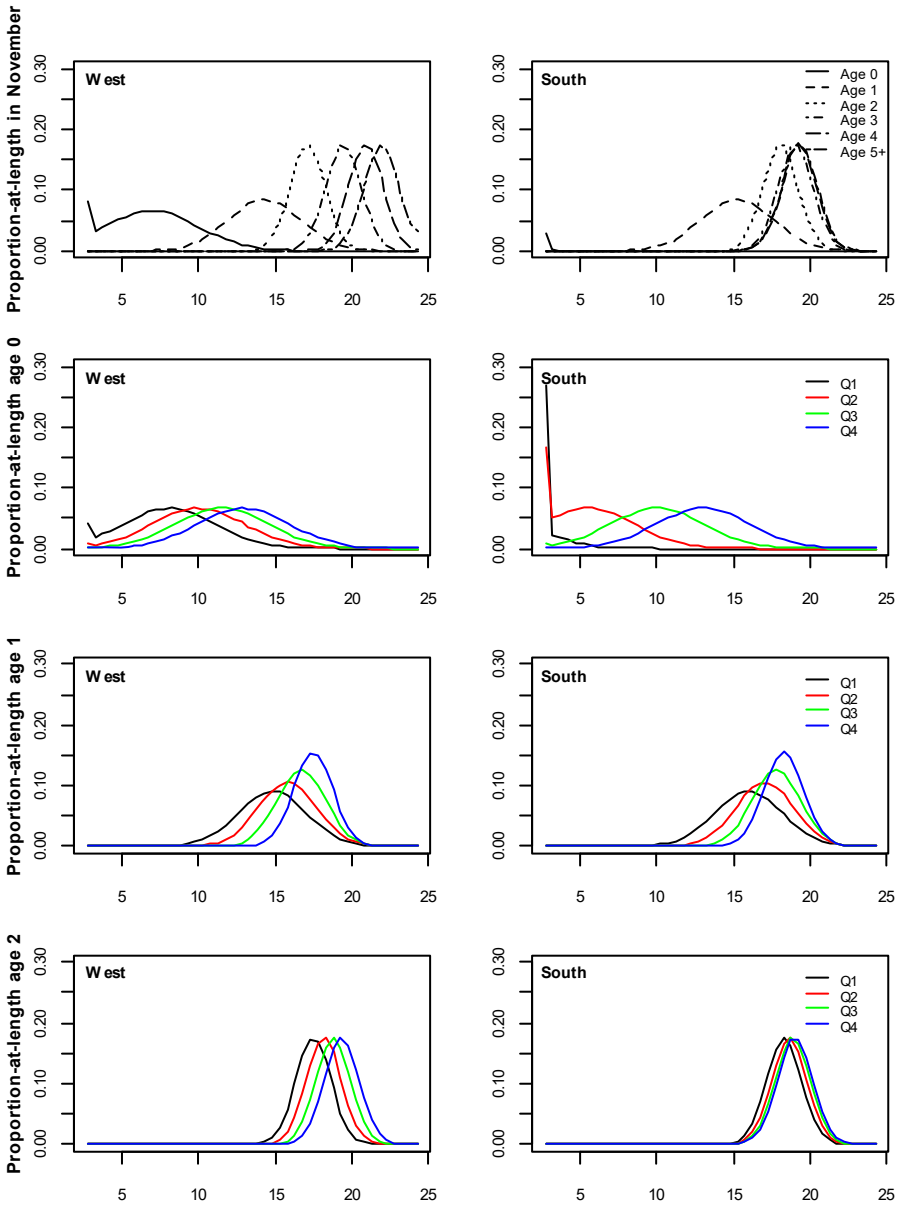

Figure 12. The model option iv) estimated distributions of proportions-at-length for each age **in 2010**, given at the time of the biomass survey (1 November, top row), and middle of each quarter of the year (corresponding to the times commercial catch is modelled to be taken) for age 0, 1 and 2 (subsequent rows).

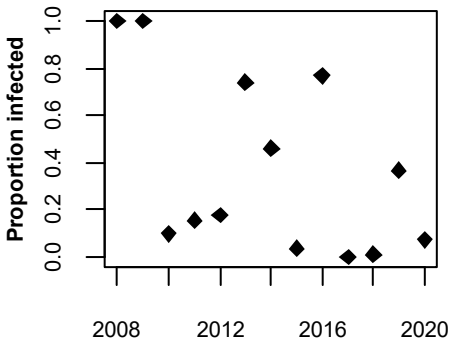

Figure 13. The model option iv) estimated proportion of west component sardine infected with the parasite between 2008 and 2020. (Annual infection rate is arbitrarily assumed to be 0 prior to 2008.)

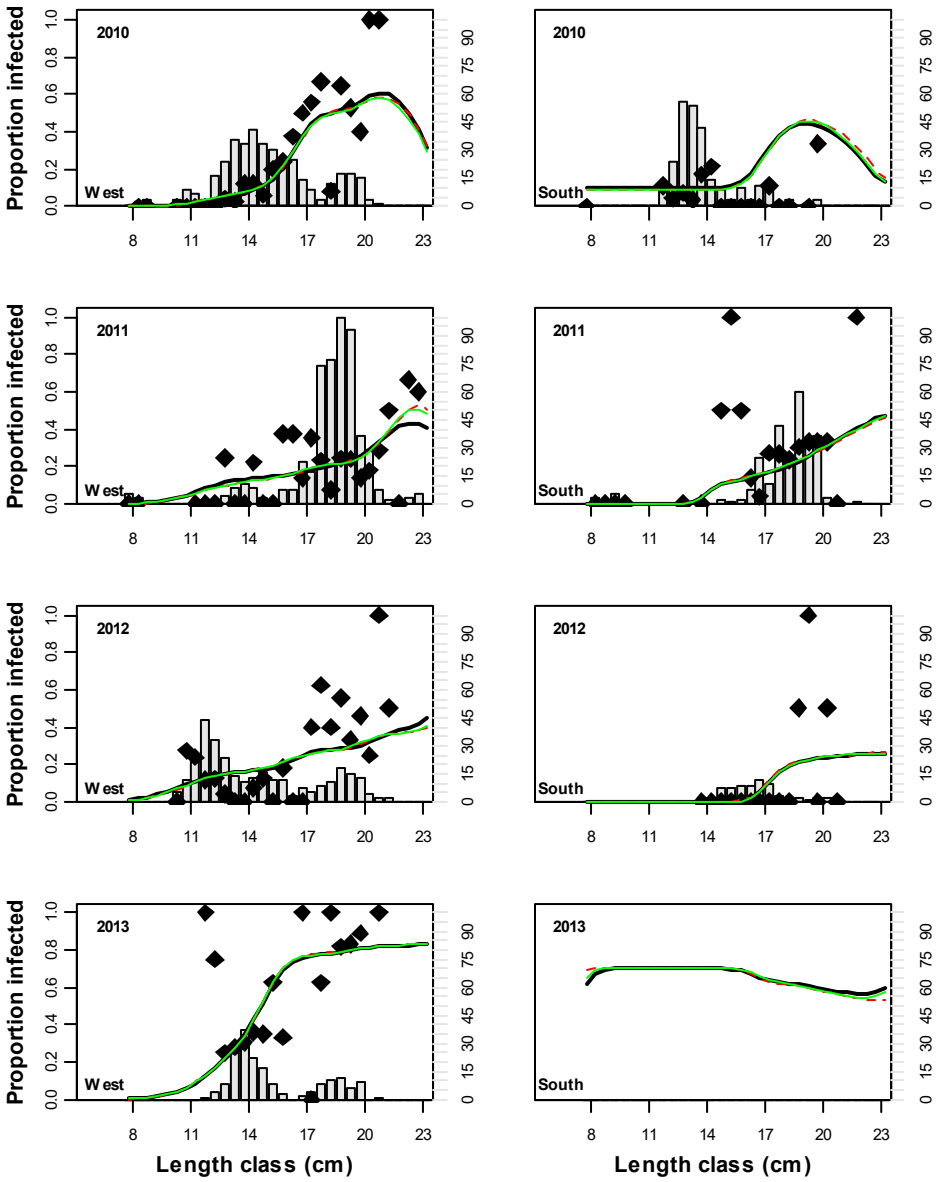

Figure 14a. The model estimated proportions-at-length of west and south stock sardine infected with the parasite (i.e. parasite prevalence-by-length) between 2010 and 2020, together with the observed proportions-at-length. Results are shown for model option iv) (black) compared to i) (green), with the red lines indicating the proportions predicted by baseline model of de Moor (2020a). The sample size for each length class is given by the grey bars, plotted against the right vertical axis.

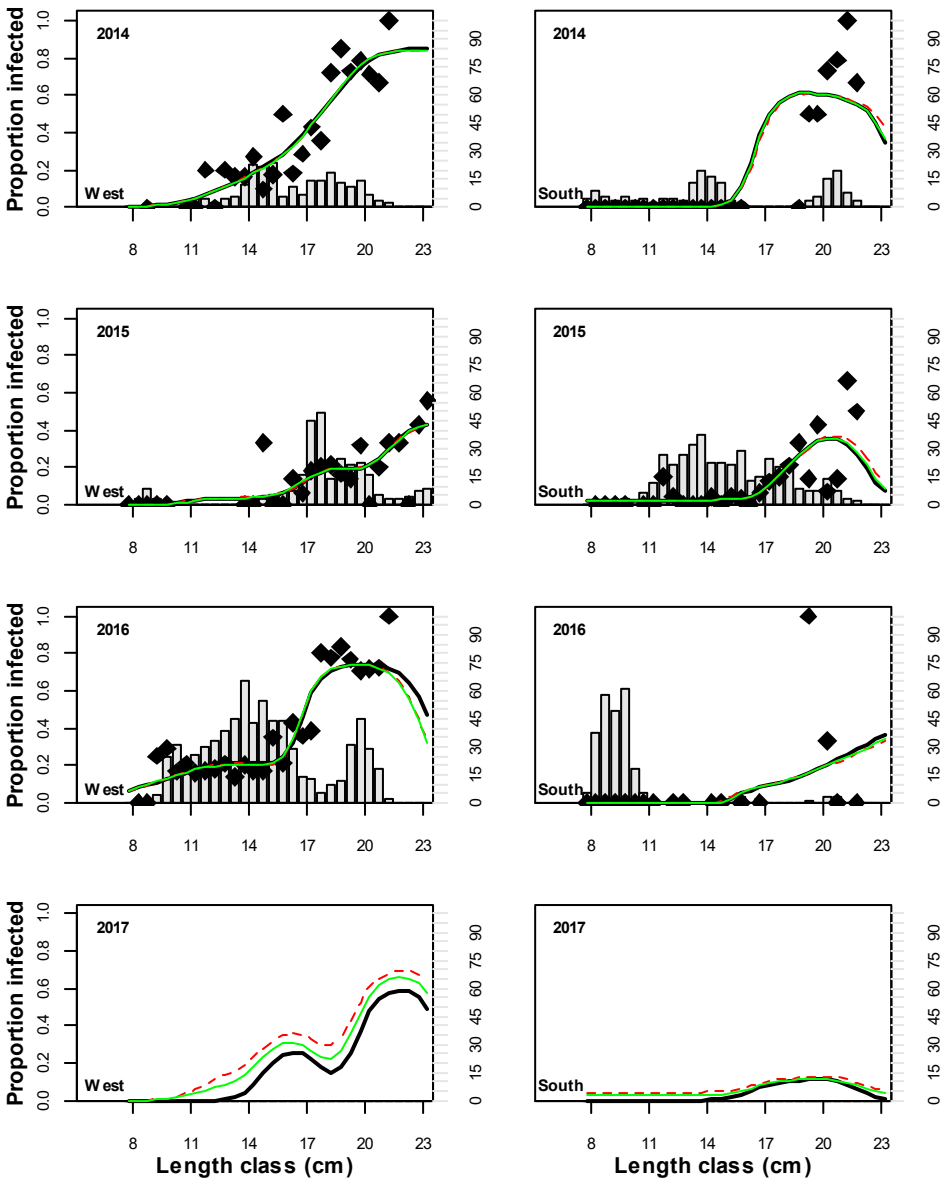

Figure 14a (continued).

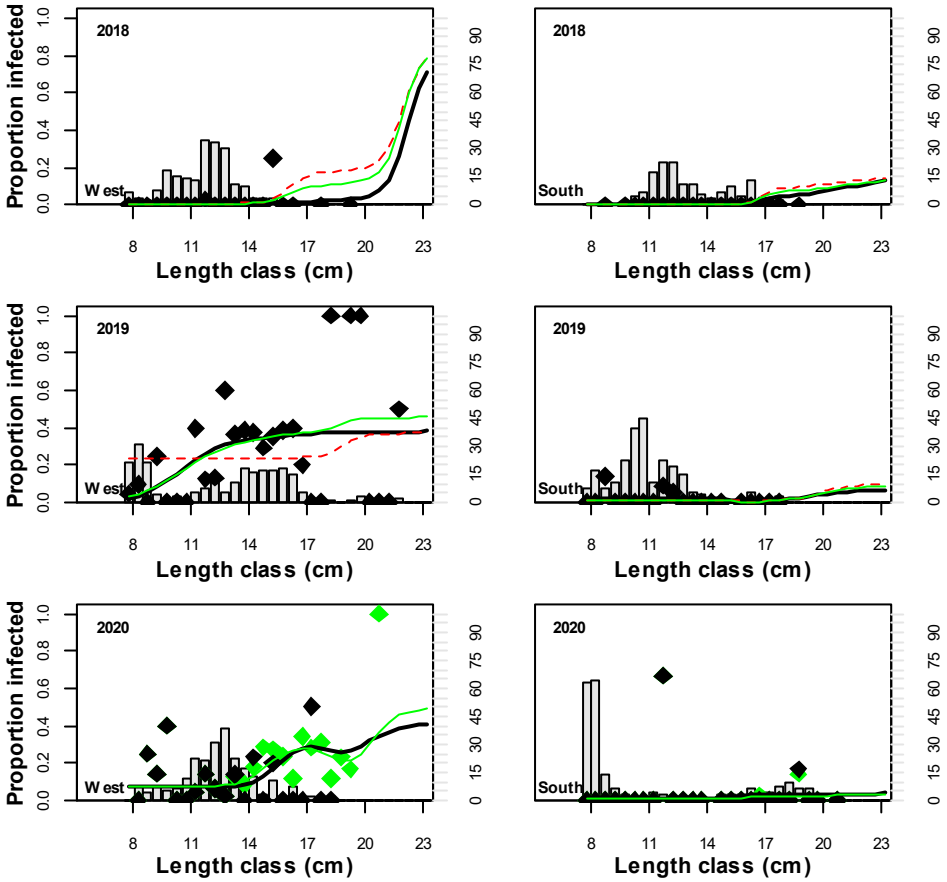

Figure 14a (continued).

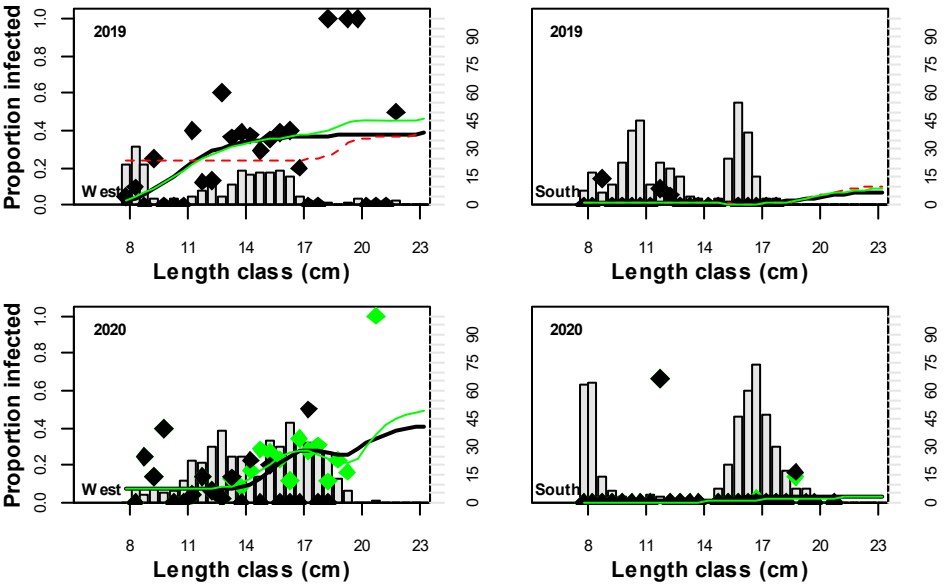

Figure 14b. As for Figure 15a for 2019 and 2020, but including the commercial samples in the observed proportions-at-length on the west (2020) and south (2019 and 2020) coasts.

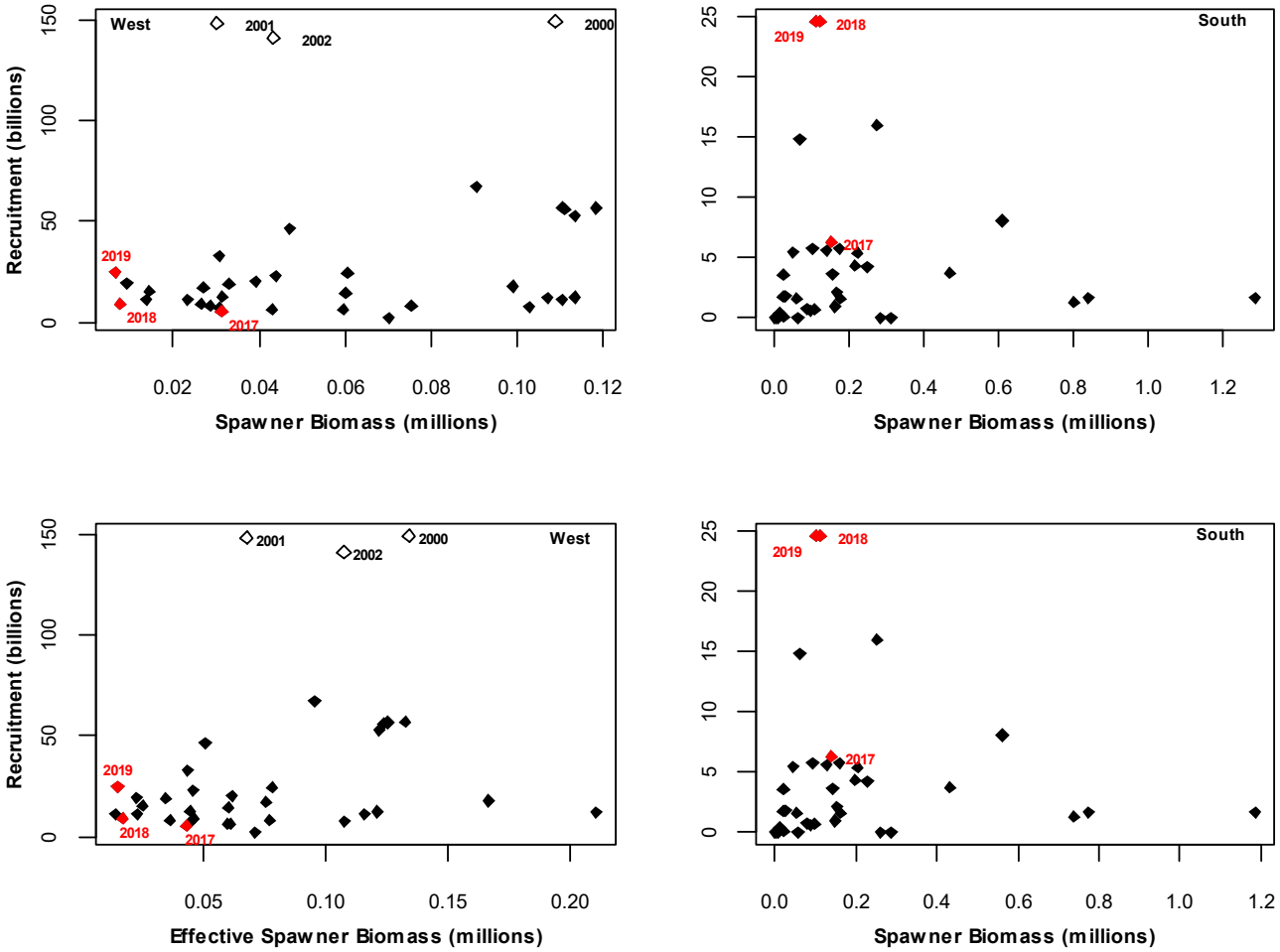

Figure 15. Model option iv) predicted sardine recruitment (in November) plotted against spawner biomass (top panels) and effective spawner biomass (lower panels) from November 1984 to November 2019. The open diamonds indicate the years of peak west component recruitment.

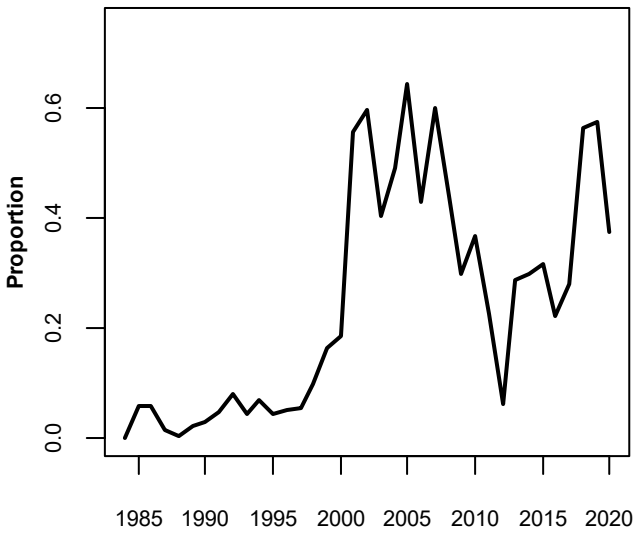

Figure 16. The proportion of west component effective spawner biomass (defined as west component spawner biomass combined with 8% of south component spawner biomass) that consists of south component spawner biomass (i.e. $SSB^{S}_{j=S,y}/SSB^{eff,S}_{j=W,y}$).

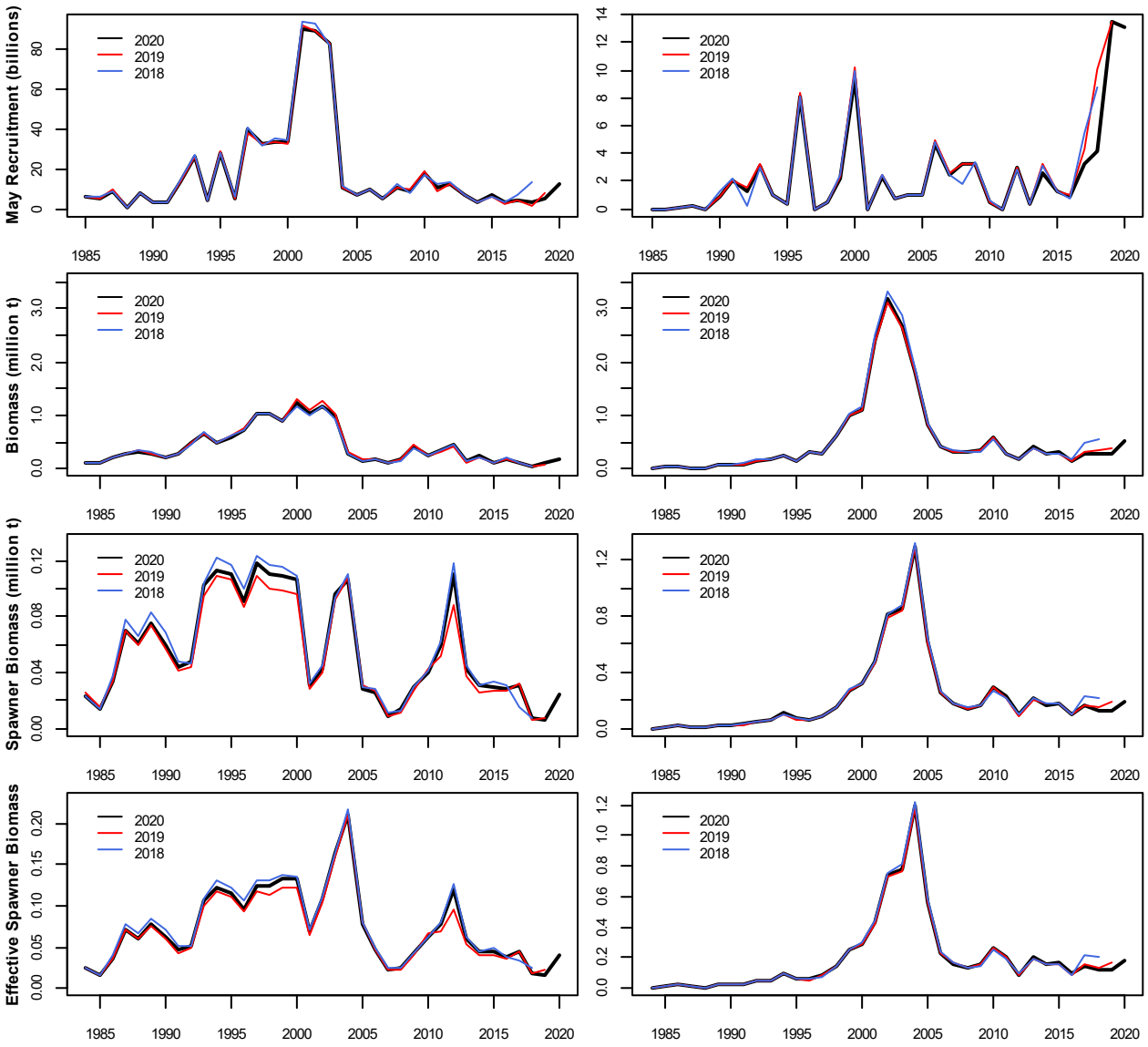

Figure 17. Model predicted May recruitment (without correction for survey bias), total biomass (without correction for survey bias), spawner biomass and effective spawner biomass and for the west and south components from model option iv) ("2020") compared to that of de Moor (2020a) ("2019") and de Moor (2020b) ("2018").

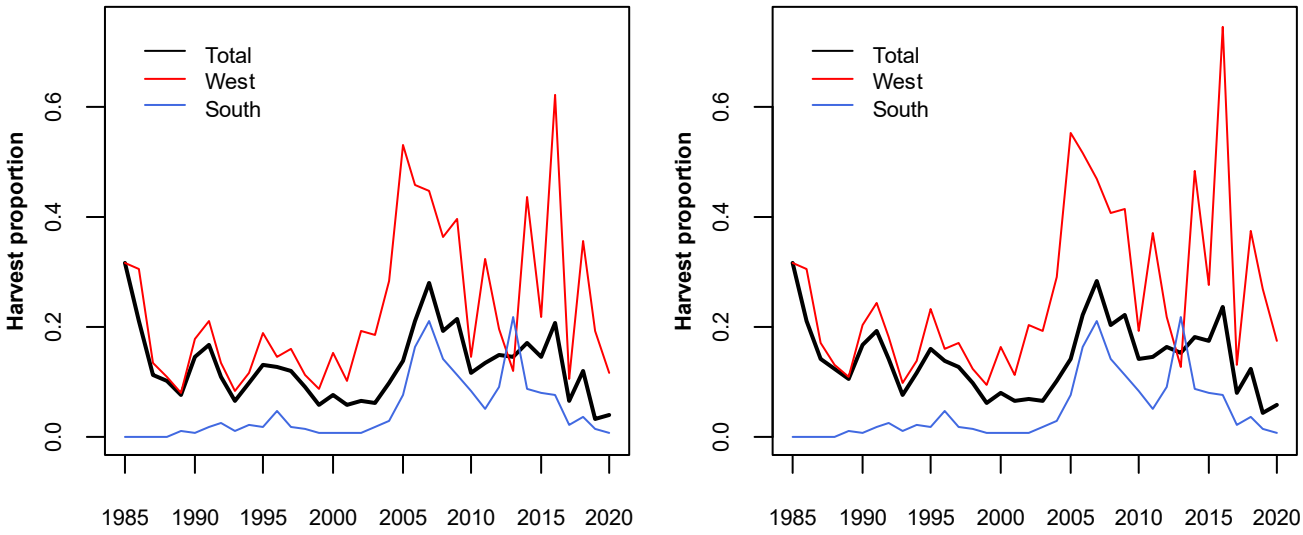

Figure 18. The exploitation rate (simply calculated as the observed annual (Nov-Oct) catch tonnage as a proportion of the model predicted total biomass). The left plot excludes small sardine bycatch with anchovy while the right plot includes these landings.